SYNTHESIS AND PROPERTIES OF NEW PARAMAGNETIC METAL-ORGANIC CAGE COMPLEXES

By

Divine Kaur Grewal

A capstone project submitted for
Graduation with University Honors

May 28, 2020

University Honors
University of California, Riverside

APPROVED

_____
Dr.Richard Hooley
Department of Chemistry

_____
Dr. Richard Cardullo, Howard H Hays Jr. Chair, University Honors

Abstract

Biomimetic reactivity is an area of research growing with creations of synthetic host molecules known as self-assembled coordination cages. These cages are unique due to their three-dimensional structure with an internal cavity capable of binding guests. This paper reports the synthesis of new paramagnetic imidazole-based-ligand cages. The new cages are synthesized using Co(II), a paramagnetic metal, that results in the broadening of the NMR spectra. This unique change to the NMR spectra is desirable because it lessens the likelihood of peak overlap. A small M2L3 cage was synthesized to create a methodology to approach making larger cages. Characterization of the small cage showed the formation of multiple species. However, when a larger M4L4 cage was then synthesized the angles of the ligand allowed for better coordination to metals, forming a discrete complex. This cage proved to be a successful host and was capable of binding steroids. The methodology reported in this paper provides an opportunity to create a wide array of new ligands with functionalization.

Introduction

An enticing area of study is self-assembled coordination cages because of their biomimetic properties and seemingly endless list of applications, including catalysis,[1] host-guest sensing,[2] and for stabilization of reactive species.[3] Enzymes are biological catalysts that can drastically accelerate rates of reactions with extreme selectivity, but are incredibly complicated and atom inefficient. Metal-organic cage complexes take inspiration from enzymes by having three dimensional structures with an internal cavity capable of binding guests. The cage's cavity provides a different environment than the surrounding solution and can be functionalized, which drives more specific guest binding. For example, a cage with a nonpolar internal cavity facilitates encapsulation of hydrophobic molecules. Supramolecular cages have analogous properties to enzymes, making them highly desirable and effective in biomimetic reactivity.

Metal-organic cages self-assemble in solution by combining simple building blocks. Iminopyridine cages combine a dianiline ligand core, metal salt and an aldehyde terminus together to form a cage complex via metal-catalyzed imine condensation (Figure 1).

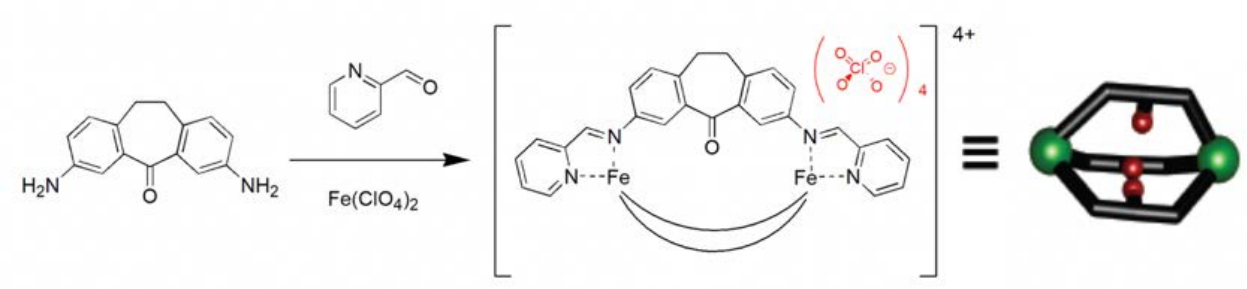

Figure 1 Iminopyridine Cage Synthesis.

Each building block can vary extensively leading to a wide array of cage structures with different characteristics. Functionalization of the ligand core by adding endohedrally oriented groups can allow the cage to be directly involved in reactions that are performed in the interior cavity.[4]

Varying the transition metal salt can introduce solubility changes[5] or paramagnetism.[6] Ligand shape and rigidity can change the cage geometry.[7-9] If a ligand is very flexible it can cause the cage to lose structural integrity. If a ligand is too rigid it can prevent complexation because of an inability of the ligand to coordinate to the metals. The combination of the components significantly influences the final cage structure and results in the most favorable complex. Intelligent design of specific building blocks allows for the characteristics of the cage complex to be controlled.

A variety of iminopyridyl ditopic cage complexes have been made by combing the building blocks stated previously.[10] Many Fe(II) cages have been synthesized with iminopyridine coordinating groups (Figure 2a). These cages have been widely studied and the effects of different anion and ligand shapes on their properties are well known. However, the limited number of available aldehyde caps limit the variability of cages. This spurs the interest in forming cages with dialdehyde ligands and amine caps because it can lead to novel functionality. Previous attempts to make dialdehyde ligand cores proved to be unsuccessful due to overoxidation. When an oxidant was added, rather than getting two aldehyde groups on the ligand, the reaction continued to form acid groups. Imidazole based ligands provide a superior method to dialdehyde ligand synthesis and open the path towards the use of amine termini. This is a highly attractive assembly process that can lead to new cages with water solubility, chirality, or covalent properties. Figure 2 shows the comparison of the two cage synthesis pathways. A methodology was created by initially forming a ditopic ligand since it resembles ditopic iminopyridine cages previously formed.[11] Once established, the methodology was applied to form more complex cages with larger internal cavities and added functionality.

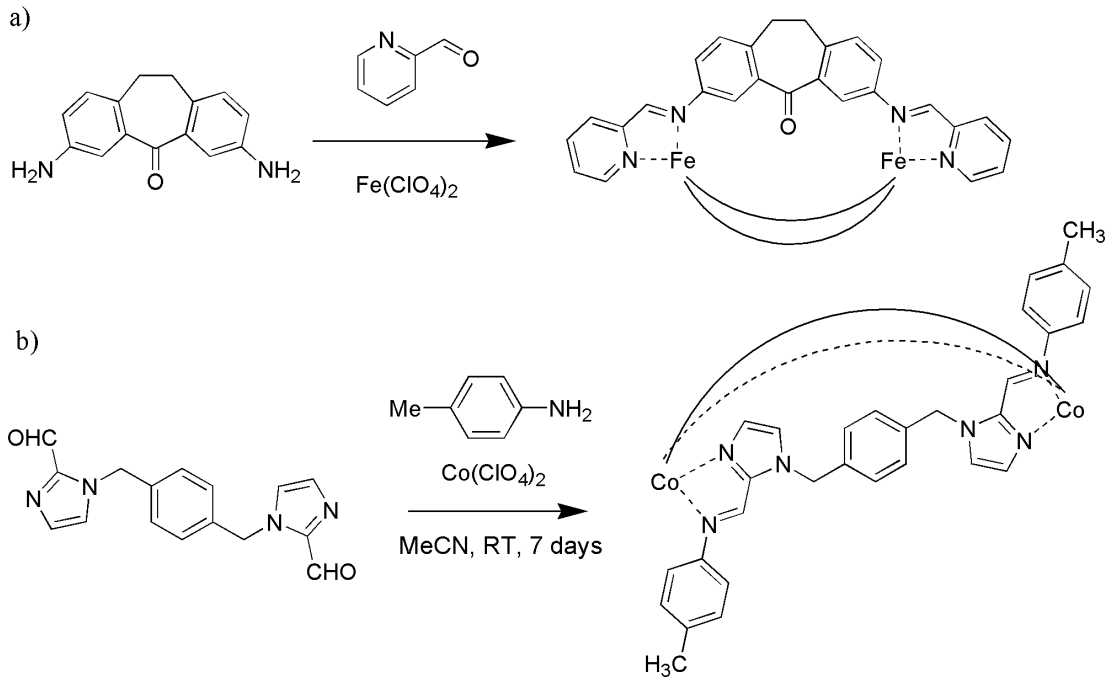

Figure 2 (a) Cage synthesis with aldehyde caps. (b) Cage synthesis with amine caps.

Paramagnetic cage complexes have altered magnetic properties based on the transition metal used in self-assembly. Octahedral transition metals that have 4-7 electrons are paramagnetic if they have an odd number of electrons in the d orbital, such as Cobalt (II).[12] Incompletely filled atomic orbitals results in a magnetic dipole moment that can act as a small magnet.[13] When paramagnetic complexes are subjected to Nuclear Magnetic Resonance (NMR) spectroscopy, the protons on the ligand that are close to a metal center are affected by both the small magnetic field of the metal and the large magnetic field of the NMR spectrometer. As a result, those protons are the most shifted peaks in the ^{1}H NMR spectrum.[14] The paramagnetic properties create distinct changes to NMR spectra including a wide chemical shift range, unreliable integration values and broadened signals.[15] Although the broadened signals lead to a loss of coupling data, these unique changes to the NMR spectra are desirable because the widened range lessens the likelihood of peak overlap and makes intermediates more apparent. This paper reports the synthesis and following

characterization of a new group of metal-organic paramagnetic imidazole-based-ligand cages. The new cages that are synthesized use Co(II), a paramagnetic metal, which results in the broadening of the NMR spectra of the complex.

Synthesis of New Compounds

Synthesizing dialdehyde ligand cores is crucial for the use of amine caps for cage assembly. The Gu group has successfully shown a method for dialdehyde ligand core formation through the use of imidazoles.[16] This synthesis uses 2-formylimidazole to form the ligand core that can combine with an amine and metal to form a coordination cage complex. This reaction is a metal mediated condensation reaction where the lone pair on the amine group can react with the carbonyl group of the aldehyde. Following this, an imine condensation occurs which results in ligand formation. The Gu group's ligand was synthesized using 1,4-dibromobutane with 2-formylimidazole. However, this synthesis results in a very flexible ligand core since it contains only alkyl groups. To produce a more stable and rigid cage structure, α, α-dibromo-p-xylene was used because it limits the degrees of freedom.

The synthesis of the ditopic ligand is shown in Figure 3a. Once the diimidazole ligand (**1**) was formed, cage formation was initially attempted with $Fe(ClO_4)_2$. This was performed because analogous complexes to imine iron cages are well known. Unfortunately, the NMR spectrum yielded broad, undistinguishable peaks indicating no complex formation. The trial led to tests of many different metals to act as coordinating groups including nickel, zinc, and cobalt. Ultimately,

the incorporation of cobalt salts, including $Co(ClO_4)_2$, proved to be the most successful in producing cage complexes with the new ligand.

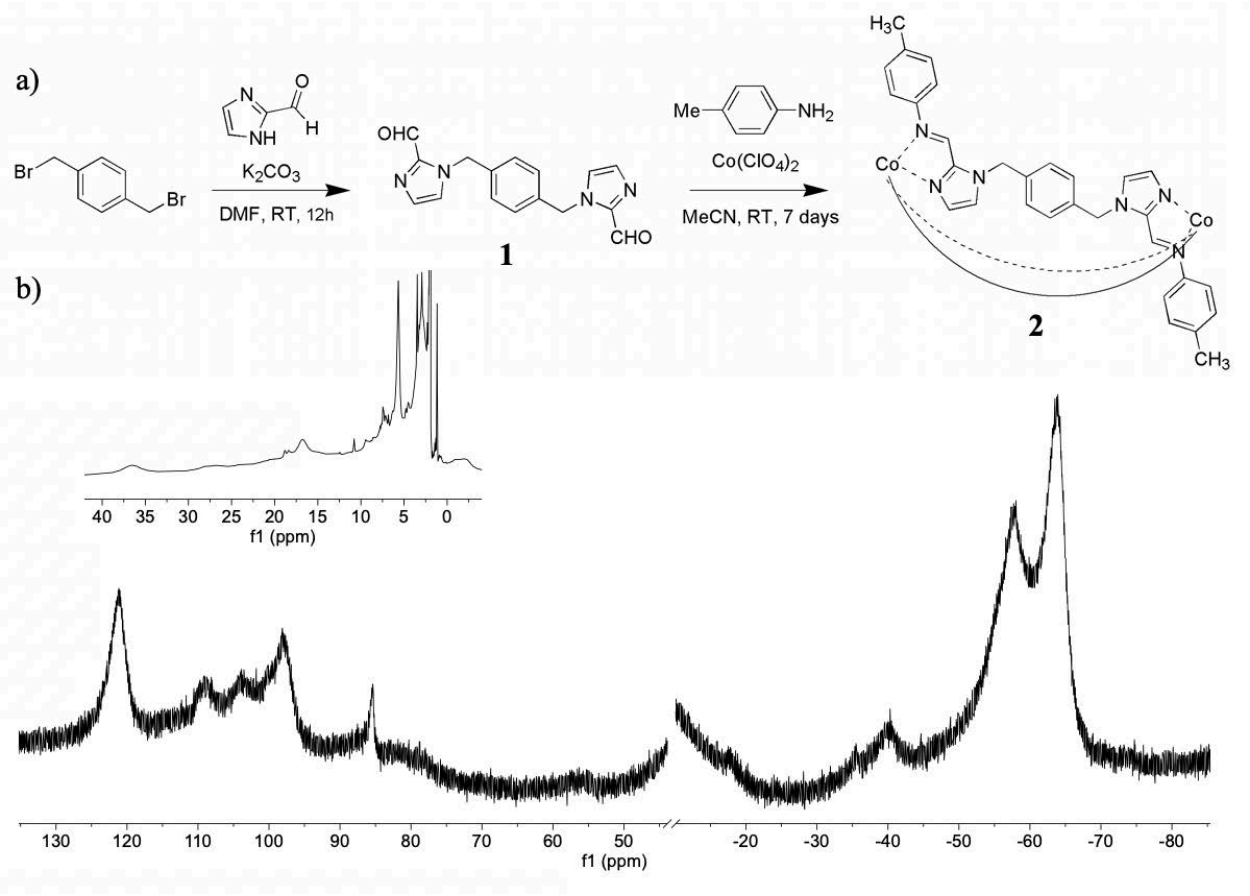

Figure 3 (a) Diimidazole ligand synthesis and multicomponent self-assembly into helicate cage complex **2**. (b) ^{1}H NMR Spectra of cage **2•ClO$_4$**.

The reaction of **1** with cobalt salt and *p*-toluidine (amine) led to the formation of paramagnetic cage complex **2** indicated by the ^{1}H NMR spectra shown in Figure 3b. Paramagnetic cage formation did occur and is indicated by the wide chemical shift range and broad peaks shown in the ^{1}H NMR. The broad peaks indicate that there are multiple species in solution, which makes it difficult to characterize the cage based on the ^{1}H NMR. ESI-MS data showed that the cage complex

formed from the ditopic ligand was a M_2L_3 helicate (Figure 4). Since the linear ligand led to the formation of multiple isomers, it was not optimal for cage formation.

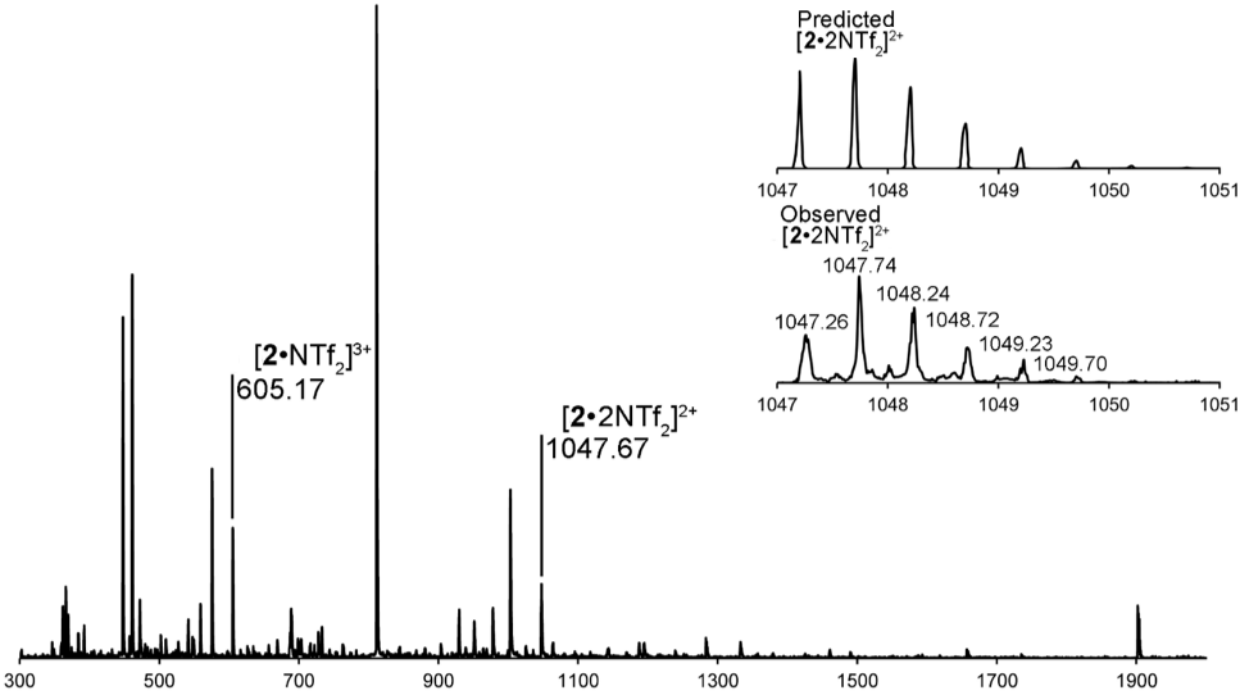

Figure 4 ESI-MS data of cage **2•NTf2**.

Using the methodology for the ditopic ligand, a tritopic ligand was synthesized to form a cage with a larger internal cavity that can be used for studying host-guest chemistry. The tritopic ligand was created in attempts to prevent multiple isomer formation. This new ligand would allow an M_4L_4 stoichiometry which has better angles for formation than the ditopic cage formation, making complexation more favorable. A tritopic ligand that can coordinate to three metals would likely

form an M_4L_4 stoichiometry and tetrahedral shape. The tritopic ligand was synthesized as shown in Figure 5.

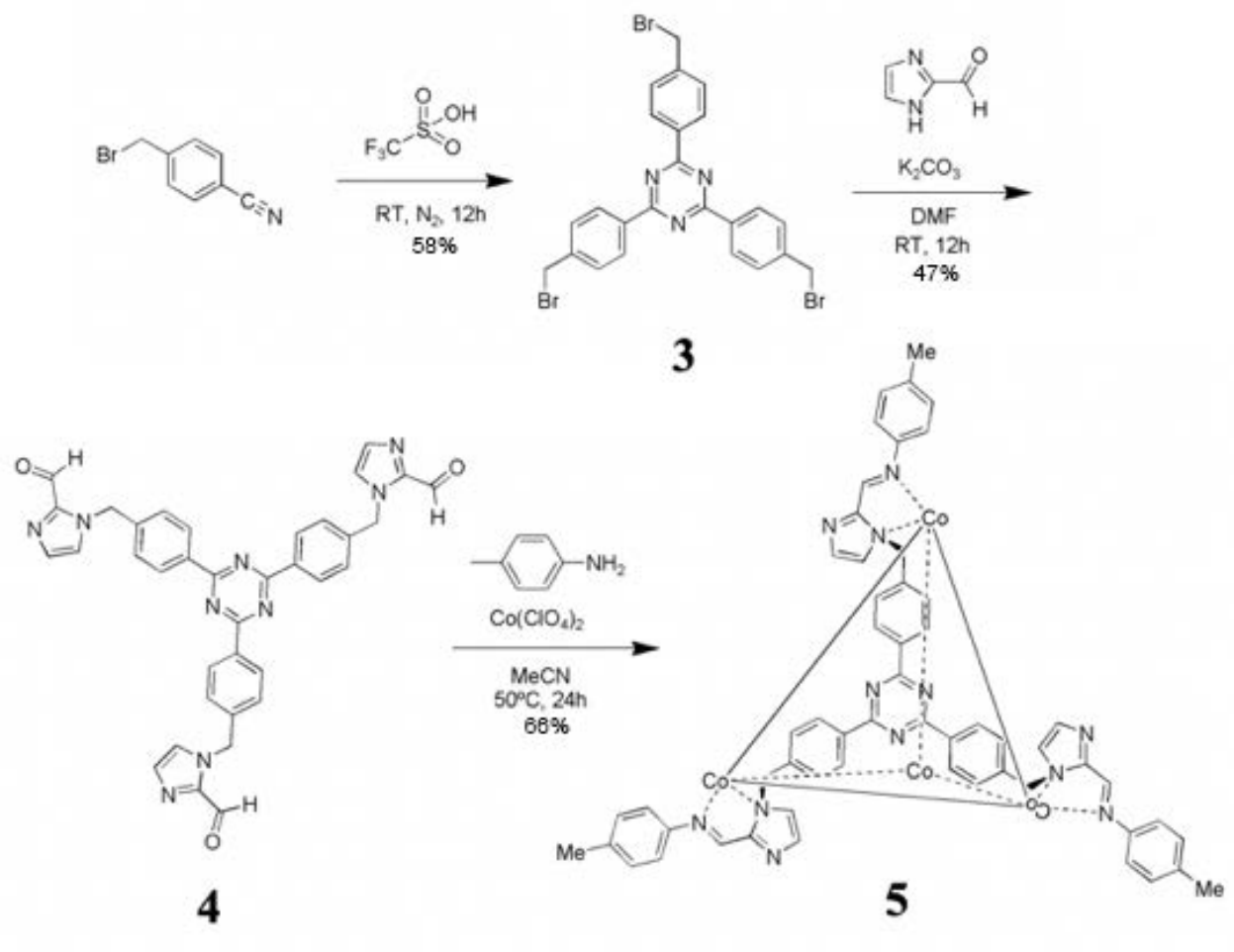

Figure 5 Triimidazole ligand synthesis and multicomponent self-assembly of tetrahedral cage **5**.

A triazine ring was formed by taking 4-cyanobenzyl bromide and reacting it with trifluoromethanesulfonic acid to form the ligand precursor **3**. Precursor **3** contains three alkyl bromide groups that are readily available to react with 2-formylimidazole and K_2CO_3 to form the rigid triimidazole ligand, **4**. Following ligand formation, cage synthesis was performed by combining **4**, *p*-toluidine, and a cobalt salt (perchlorate, ClO_4, or triflimide, NTf_2). Unlike cage **2**, the NMR spectra of the triimidazole cages showed sharp, distinguishable peaks. NMR spectra for

the triimidazole cobalt cage (**5**) indicated the formation of a discrete paramagnetic cage based on the wide distribution of relatively sharp peaks in the spectrum (Figure 6 b, c). Surprisingly, while the reaction conditions were identical, the NMR spectra of cage **5•ClO_4** showed the formation of one isomer because there is only one set of peaks present, whereas cage **5•NTf_2** showed six sets

of peaks indicating formation of multiple isomers. The differences in isomer formation can possibly be attributed to anion templation. Anions can vary in shape and range of coordination geometries which can help direct the self-assembly of cages. In many cases, the anion aids in organization and can help reduce the number of isomers formed. The perchlorate anion is driving

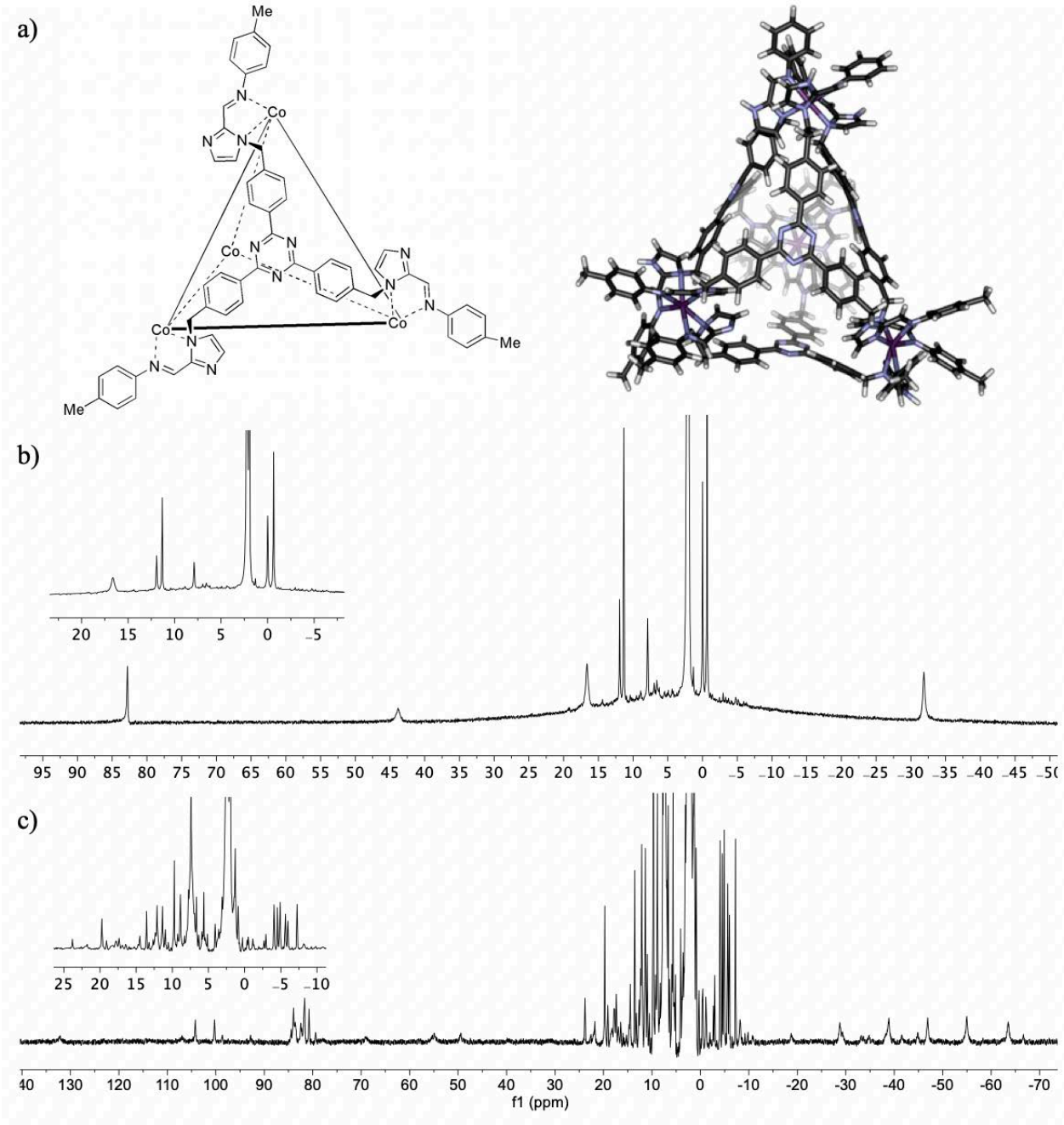

Figure 6 (a) Minimized structure of cage **5**. (b) ^{1}H NMR spectra of cage **5•ClO$_4$**. (c) ^{1}H NMR spectra of cage **5•NTf$_2$**.

the formation of one isomer. Based on the NMR spectra of **5•ClO$_4$** versus **5•NTf$_2$**, it was unclear if the cages were similar since the change in anion could cause different symmetry formation. Analysis of the cages through ESI-MS were performed (Figure 7). The data showed similar fragmentation patterns and confirmed the stoichiometry of the cages as M_4L_4 tetrahedra.

To confirm the cage structures, coordination and symmetry, X-ray diffraction analysis of a single crystal must be performed. To crystallize cage **5•NTf$_2$**, slow vapor diffusion of various

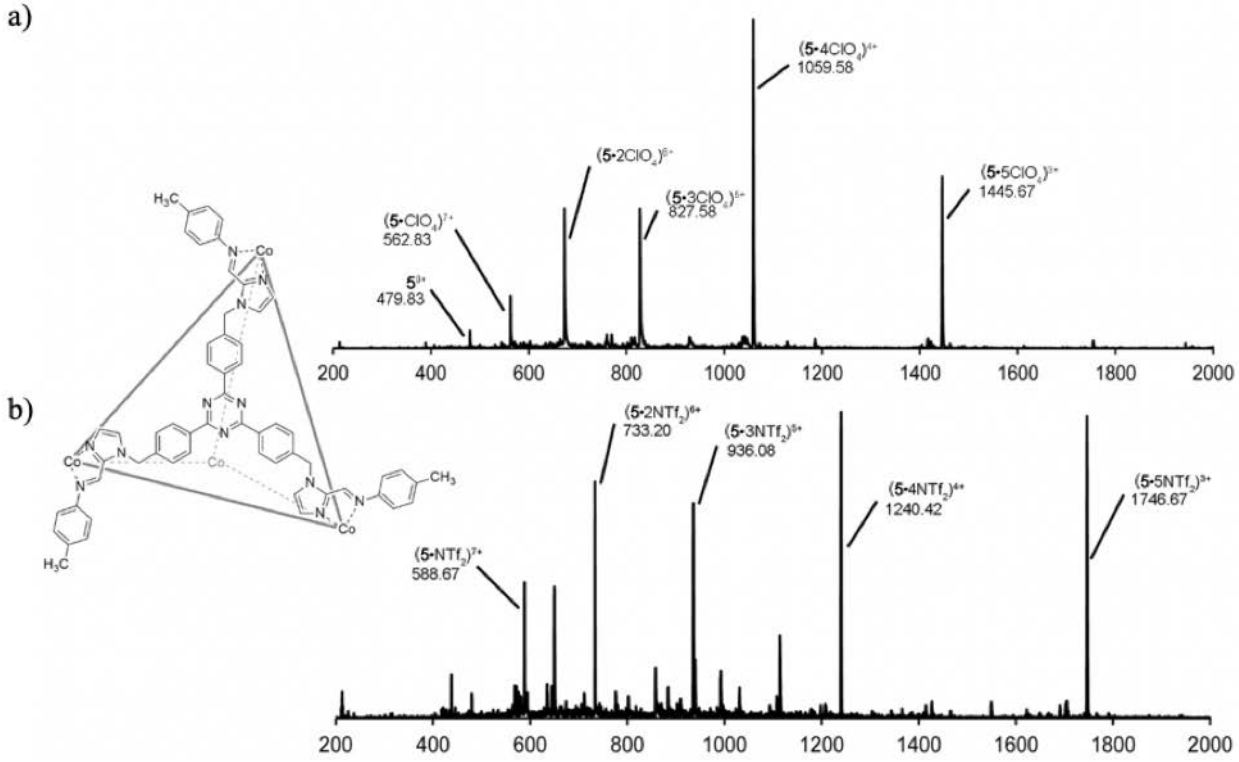

Figure 7 ESI-MS data of cages (a) **5•ClO$_4$** (b) **5•NTf$_2$**.

ethers into a solution of **5•NTf$_2$** and acetonitrile were performed. The ethers that were diffused included diethyl ether, isopropyl ether, and methyl tert-butyl ether. The trials did not form suitable crystals. Diffusion of isopropyl ether was the most promising, but crystals of the salt were present. Purification methods and iterative recrystallization yielded thicker needles than initially formed but they were unable to be diffracted.

Anion Exchange

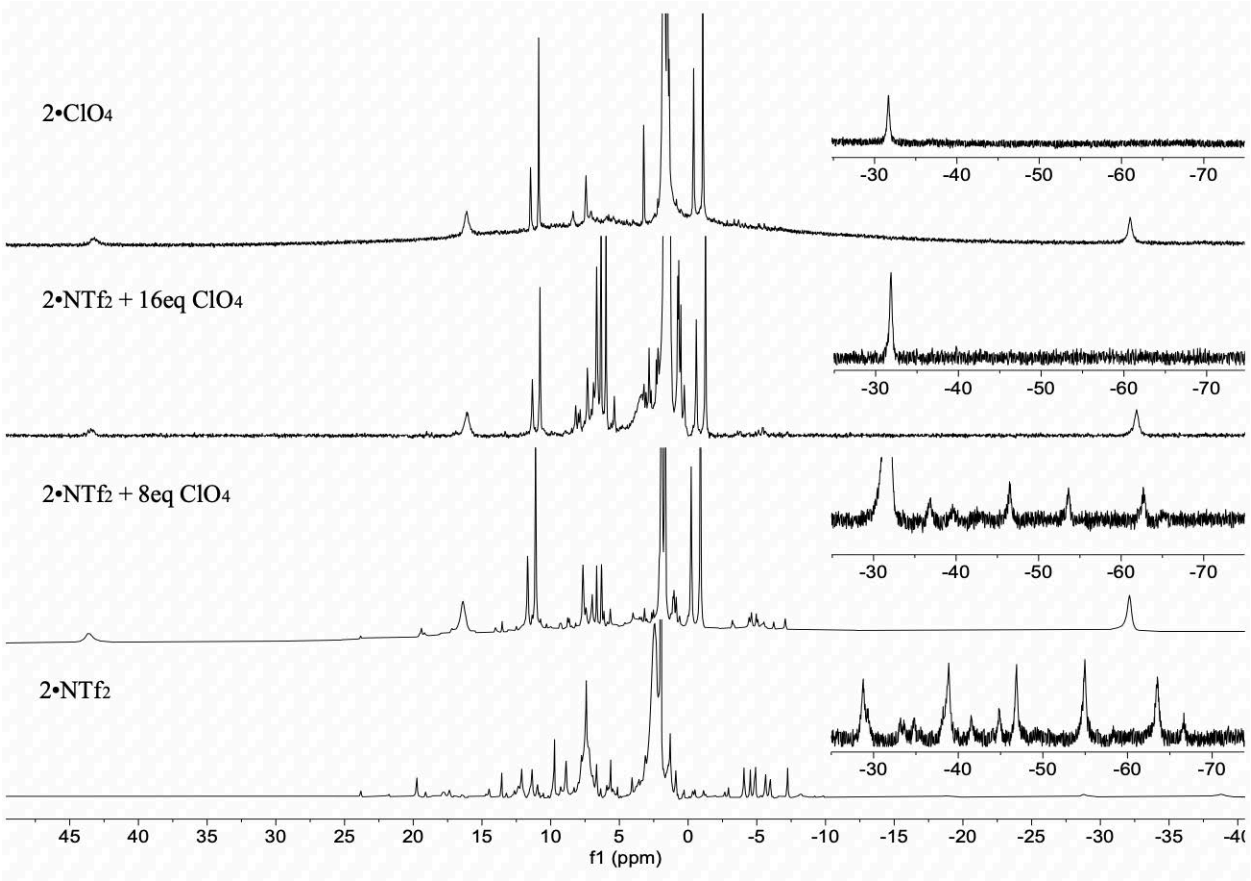

Figure 8 Anion exchange from **5•NTf$_2$** (bottom) to **5•ClO$_4$** (top), with magnification from -25 to -75 ppm.

Cage **5** formed complexes with both perchlorate and triflimide cobalt anions. In order to determine which anion was more favorable, a comparative anion exchange study was performed. The ^{1}H NMR data showed that **5•ClO$_4$** formed a single isomer, indicated by one set of peaks, however **5•NTf$_2$** showed multiple sets of peaks. Based on the number of isomers forming in each case, it was initially assumed that cage **5•ClO$_4$** was more energetically favorable. To test this assumption, perchlorate anions from $NaClO_4$, were added to a solution of **5•NTf$_2$** (Figure 8). When this was performed, the ^{1}H NMR showed that the spectra changed because some peaks corresponding to **5•ClO$_4$** formed. The addition of 8 equivalents of ClO_4^- anion resulted in many of

the **5•NTf$_2$** peaks dropping out. However, there were still peaks of **5•NTf$_2$** that remained showing it did not completely change. Similarly, when the reverse experiment was performed, $NaNTf_2$ was added to a solution of **5•ClO$_4$**, many paramagnetic peaks began to form. The tests indicated that neither complex was more energetically favored, rather an equilibrium was reached between the two.

Binding Studies via UV-vis Titrations

Cage **5**, structurally, has a cavity large enough to act as a host and encapsulate small guests. A variety of small molecules were tested, by UV-vis titration, to determine what the cage could bind. Isosbestic points in a UV-vis curve indicate binding of the guest into the host cavity. Tests were performed with small organic molecules including aromatics (pyrene and anthracene) and steroids (progesterone, estrone, and estradiol). Cage **5•ClO$_4$** did not successfully encapsulate any of the guest molecules because there were no isosbestic points shown in the UV-vis titration curves. Cage **5•NTf$_2$** did not show complex formation with the small aromatic molecules. However, isosbestic points were formed with the addition of progesterone and estrone (Figure 9).

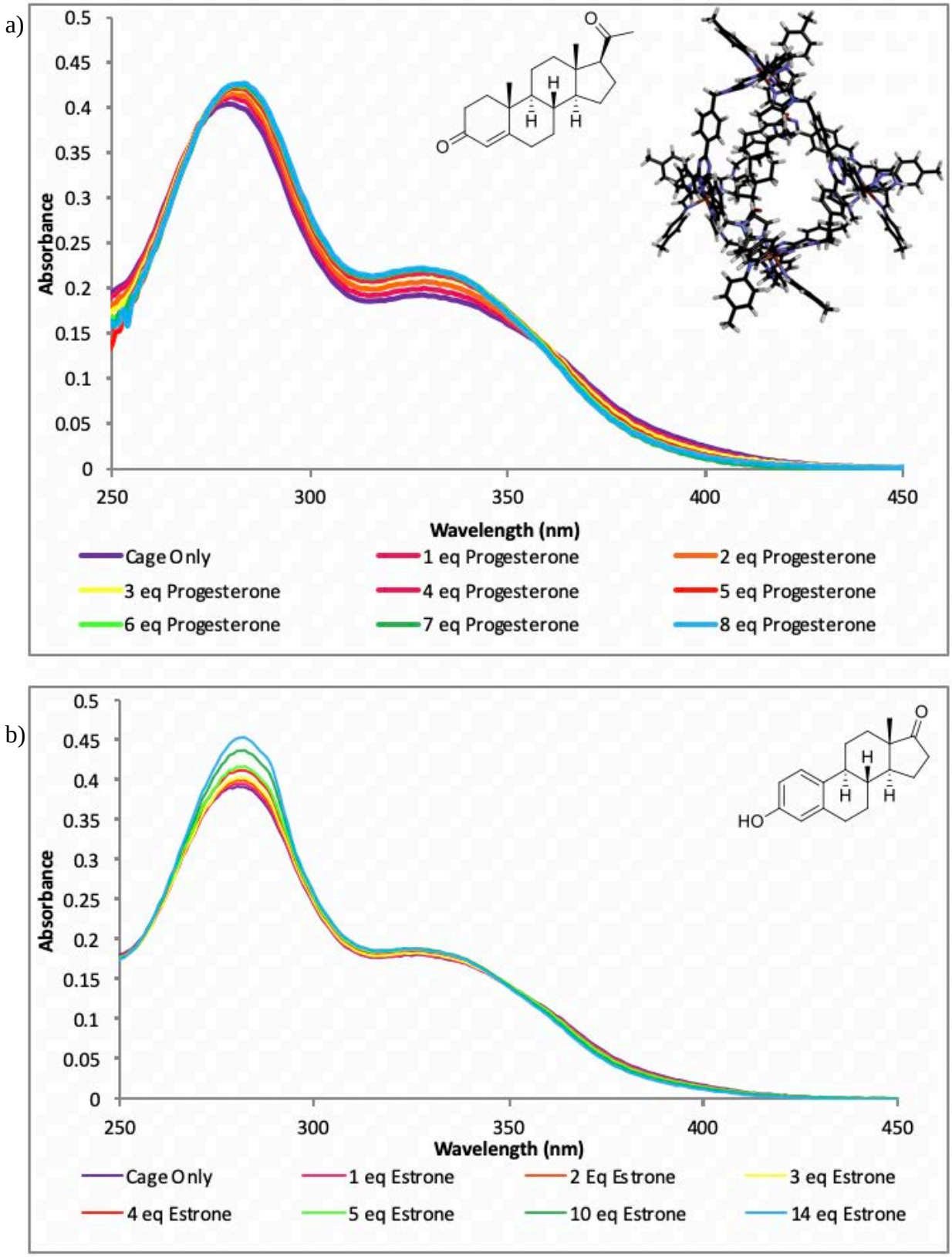

Figure 9 UV-vis titration curves of **5•NTf$_2$** with (a) progesterone with energy minimized SPARTAN model of progesterone inside cage **5** and (b) estrone.

Conclusion

This paper reported the synthesis of new paramagnetic metal-organic cage complexes. The imidazole ligand assembly process provides an opportunity to create a wide variety of new ligands. The ditopic ligand and cage, **2•ClO$_4$**, that was created established the methodology that can be applied to create larger cage complexes. This process led to the assembly of paramagnetic cages **5•ClO$_4$** and **5•NTf$_2$**. Cage **5•NTf$_2$** was successful in anion exchange and host-guest chemistry. Its properties can be further studied and used as a template to add functionalization on the triazine core moiety. While crystal structures were unattainable for **5•NTf$_2$**, the use of NMR spectroscopy and mass spectrometry allowed for structure determination. Anion exchange studies of cage **5** showed that there was no preference based on energetic favorability. Instead, there was an equilibrium bias between the two anions. UV-vis titrations showed that cage **5•NTf$_2$** has the ability of binding some small steroid molecules. Further host-guest studies and crystallization attempts on these paramagnetic cage complexes will be ongoing.

Experimental Section

General Information

^{1}H, and ^{13}C spectra were recorded on Bruker Avance NEO 400 or Bruker Avance 600 MHz NMR spectrometer. Proton (^{1}H) and carbon (^{13}C) chemical shifts are reported in parts per million (δ) with respect to tetramethylsilane (TMS, δ=0), and referenced internally with respect to the protic solvent impurity for CD_3CN (^{1}H: 1.94 ppm, ^{13}C: 118.26). Deuterated NMR solvents were obtained from Cambridge Isotope Laboratories, Inc., Andover, MA, and used without further purification. Spectra were processed (phase and baseline corrections, integration, peak analysis) using Bruker Top-spin 1.3 and MestreNova. Mass spectrometric samples were infused into an Orbitrap Velos Pro mass spectrometer with the standard HESI source at a flow rate of 3 μL/min.

The spray voltage was 3 kV, capillary temperature was set to 170 °C and an S-lens RF level of 45 % was applied. Full FTMS were acquired with a resolution of r = 30,000, and ambient ions were used as internal lock mass calibrants. CID spectra were collected in ZoomScan mode where the isolation window = 5 m/z, normalized collision energy (nCE) = 30 and activation time = 30 ms. MS data was analyzed using Thermo XCalibur. Predicted isotope patterns were prepared using ChemCalc. UV/Vis spectroscopy was performed on a Cary 60 Photo-spectrometer by using the Varian Scans program to collect data. All other materials were obtained from Aldrich Chemical Company (St. Louis, MO), or Fisher Scientific (Fairlawn, NJ), and were used as received. Solvents were dried through a commercial solvent purification system (Pure Process Technologies, Inc.).

Synthesis of (1)

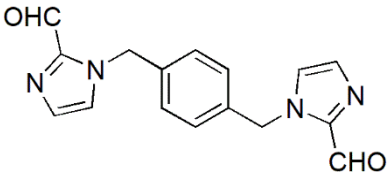

In a 50 mL two neck round bottom flask with a stir bar the following were combined: α, α-dibromo-p-xylene (400 mg, 1.50 mmol) with 2-imidazolecarboxaldehyde (393 mg, 4.09 mmol) and K_2CO_3 (394 mg, 2.85 mmol). The flask was purged with N_2. Dry DMF (2 mL) was injected into the flask via syringe. The reaction was stirred at ambient temperature for 12 h. The reaction was then titrated with hexanes and the solid was filtered. The filtered solid was dissolved in 30 mL CH_2Cl_2. The solution was extracted three times with 20 mL concentrated $NaHCO_3$ solution followed by 15 mL brine. The organic solution was then dried with $MgSO_4$ and filtered. The remaining solvent was removed in a vacuum leaving a white powder (63%).

^{1}H NMR (400 MHz, $CDCl_3$) δ 9.84 (q, *J* = 2.7 Hz, 2H), 7.33 (d, *J* = 4.5 Hz, 2H), 7.20 – 7.17 (m, 4H), 7.16 (d, *J* = 3.8 Hz, 2H), 5.62 – 5.59 (m, 4H).

Synthesis of 2,4,6-tris(4-(bromomethyl)phenyl)-1,3,5-triazine (3)

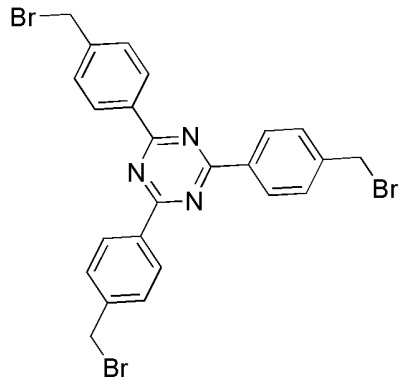

In a 100 mL Schlenk flask with a stir bar, 4-cyanobenzyl bromide (1.00 g, 5.1 mmol) was added. The flask was purged with N_2 and brought to 0°C in an ice bath. Trifluoromethanesulfonic acid (1.35 mL, 5.1 mmol) was then added slowly to the flask via syringe and purged again. Once addition was complete, the flask was removed from the ice bath and allowed to warm to ambient temperature (color turned orange). The solution was then stirred at room temperature for 12 h. The mixture was poured over ice-cold water forming a white precipitate which was then filtered and washed with acetone to yield a white solid (58%).

^{1}H NMR (400 MHz, $CDCl_3$) δ 8.72 (d, *J* = 8.0 Hz, 6H), δ 7.62 (d, *J* = 8.0 Hz, 6H), 7.34 (s, 1H), 4.61 (s, 6H).

Synthesis of (4)

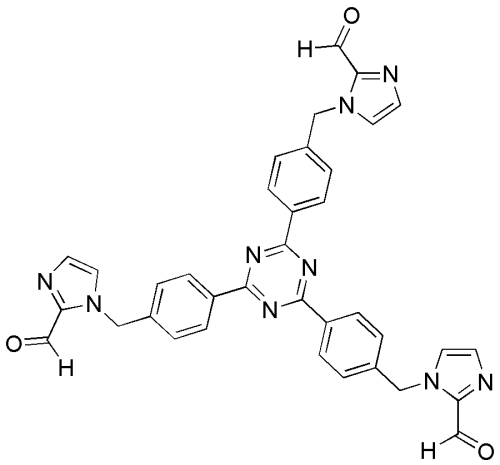

In a 50 mL two neck flask with stir bar **3** (300 mg, 0.51 mmol), 2-imidazolecarboxaldehyde (198.6 mg, 2.07 mmol), and K_2CO_3 (201 mg, 1.5 mmol) were combined. The flask was purged with N_2 and dry DMF (2 mL) was then added into the flask via syringe. The reaction stirred for 12 h at ambient temperature. Then, the reaction was titrated with hexanes producing a solid precipitant. The solid was filtered and dissolved in 30 mL DCM. The solution was extracted three times with 20 mL of concentrated $NaHCO_3$ solution followed by 15 mL brine. The organic solution was then dried with $MgSO_4$ and filtered. The remaining solvent was removed by vacuum leaving a white powder (47%).

^{1}H NMR (400 MHz, $CDCl_3$) δ 9.89 (d, *J* = 1.0 Hz, 1H), 8.78 – 8.66 (m, 2H), 7.38 (dd, *J* = 4.7, 3.7 Hz, 3H), 7.24 (d, *J* = 1.1 Hz, 1H), 5.75 (s, 2H).

Synthesis of Diimidazole Cage (2•ClO_4)

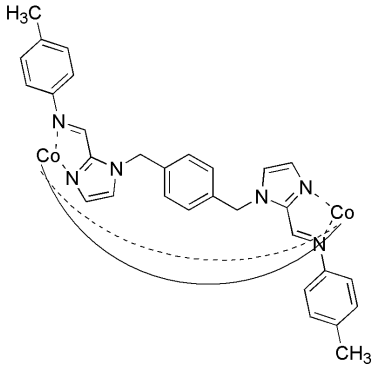

In a 50 mL two neck flask with stir bar **1** (30 mg, 0.102 mmol), $CoClO_4$ (37.3 mg, 0.102 mmol), and *p*-toluidine (21.9 mg, 0.204 mmol) were combined. The flask was purged with N_2 and then MeCN (5 mL) was added via syringe. The mixture reacted at 50°C for 2 days. Solvent was removed *in vacuo,* then titrated with ether and filtered. The solid was washed with 1:1 methanol: ether (10 mL) resulting in a reddish brown solid (59%). See Figure 15 for ^{1}H NMR spectrum.

Synthesis of Diimidazole Cage (2•NTf_2)

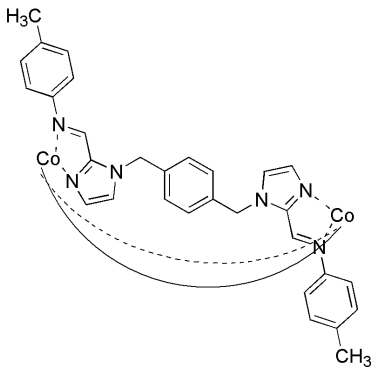

In a 50 mL two neck flask with stir bar **1** (30 mg, 0.102 mmol), $Co(NTf_2)_2$ (63.2 mg, 0.102 mmol), and *p*-toluidine (21.9 mg, 0.204 mmol) were combined. The flask was purged with N_2 and then MeCN (5 mL) was added via syringe. The mixture reacted at 50°C for 2 days. Solvent was removed *in vacuo,* then titrated with ether and filtered. The solid was washed with 1:1 methanol: ether (10 mL) resulting in a reddish brown solid (64%). See Figure 16 for ^{1}H NMR spectrum.

Synthesis of Triimidazole Cage (5•ClO_4)

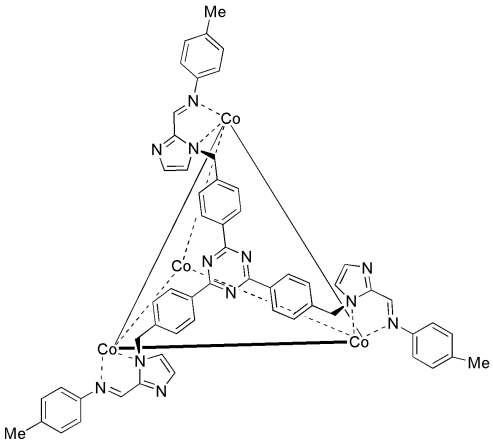

In a 50 mL two neck flask with stir bar **4** (50 mg, 0.079 mmol), $CoClO_4$ (28.7 mg, 0.079 mmol), and *p*-toluidine (25 mg, 0.237 mmol) were combined. The flask was purged with N_2 and MeCN (5 mL) was added via syringe. The mixture reacted at 50°C for 2 days. Solvent was removed *in vacuo*, then titrated with ether and filtered. The solid was washed with 1:1 mixture of methanol: ether (10 mL) resulting in a reddish brown solid (66%). See Figure 17 for ^{1}H NMR spectrum.

Synthesis of Triimidazole Cage (5•NTf_2)

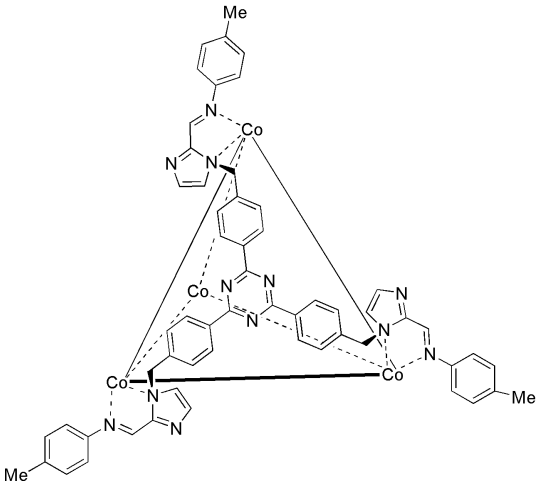

In a 50 mL two neck flask with stir bar **4** (50 mg, 0.079 mmol), $Co(NTf_2)_2$ (49 mg, 0.079 mmol), and *p*-toluidine (25 mg, 0.237 mmol) were combined. The flask was purged with N_2 and MeCN (5 mL) was added via syringe. The mixture reacted at 50°C for 2 days. Solvent was removed *in*

vacuo, then titrated with ether and filtered. The solid was washed with 1:1 mixture of methanol: ether (10 mL) resulting in a reddish brown solid (64%). See Figure 18 for ^{1}H NMR spectrum.

NMR and ESI-MS Characterization of New Cage Compounds and Precursors

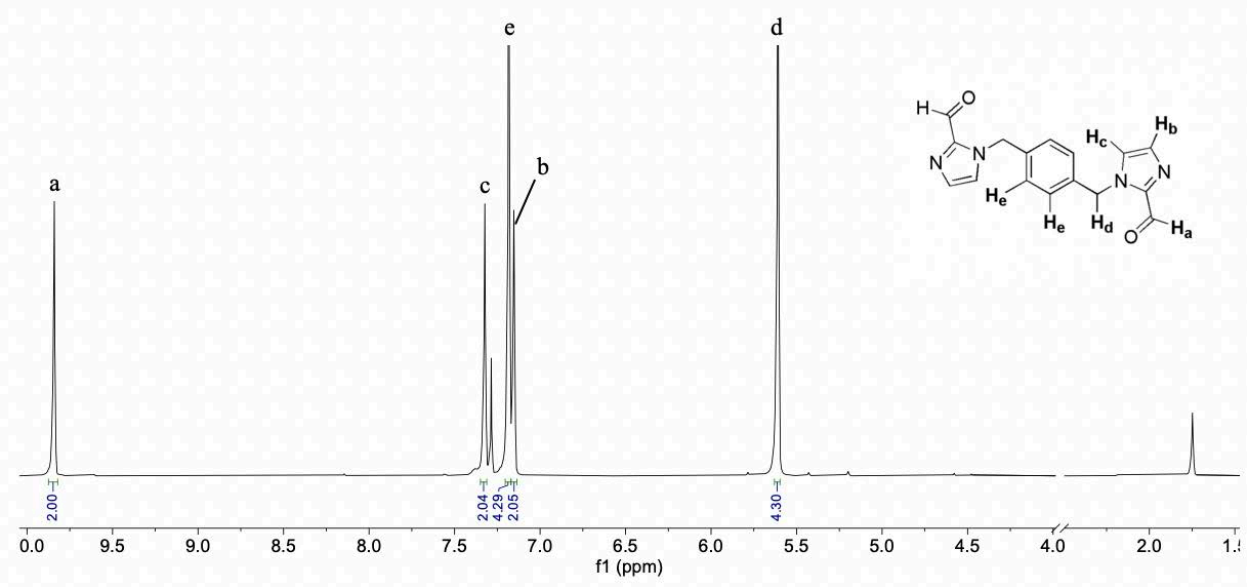

Figure 10 ^{1}H NMR Spectrum of Diimidazole Ligand **1** ($CDCl_3$, 400 MHz, 298 K).

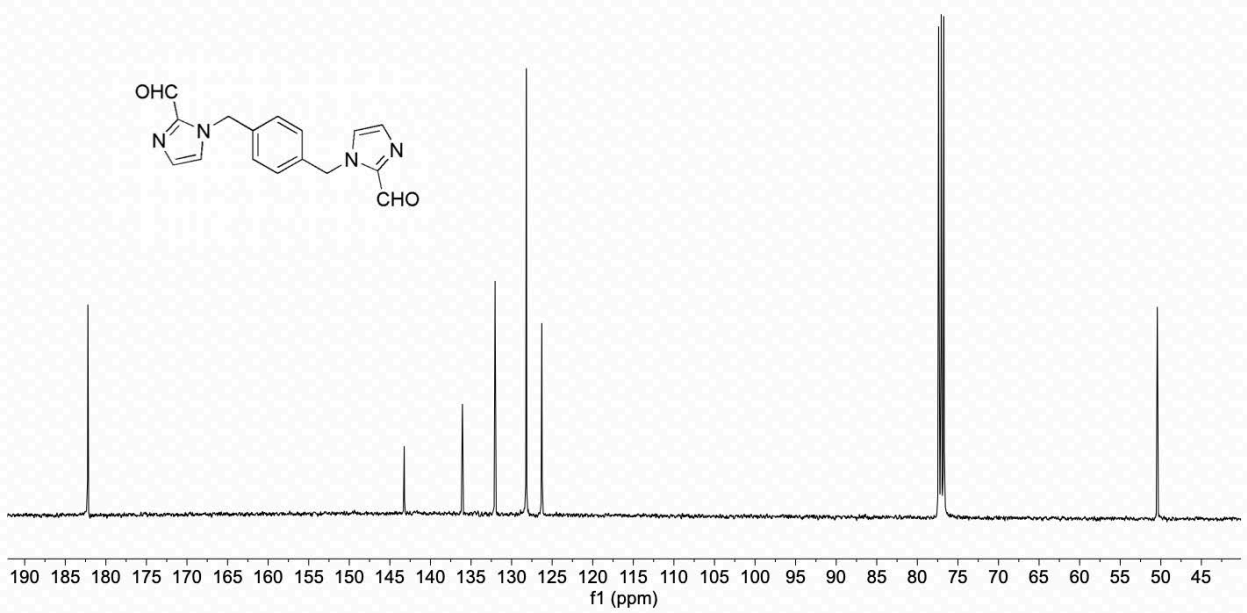

Figure 11 ^{13}C NMR Spectrum of Diimidazole Ligand **1** ($CDCl_3$, 101 MHz, 298 K).

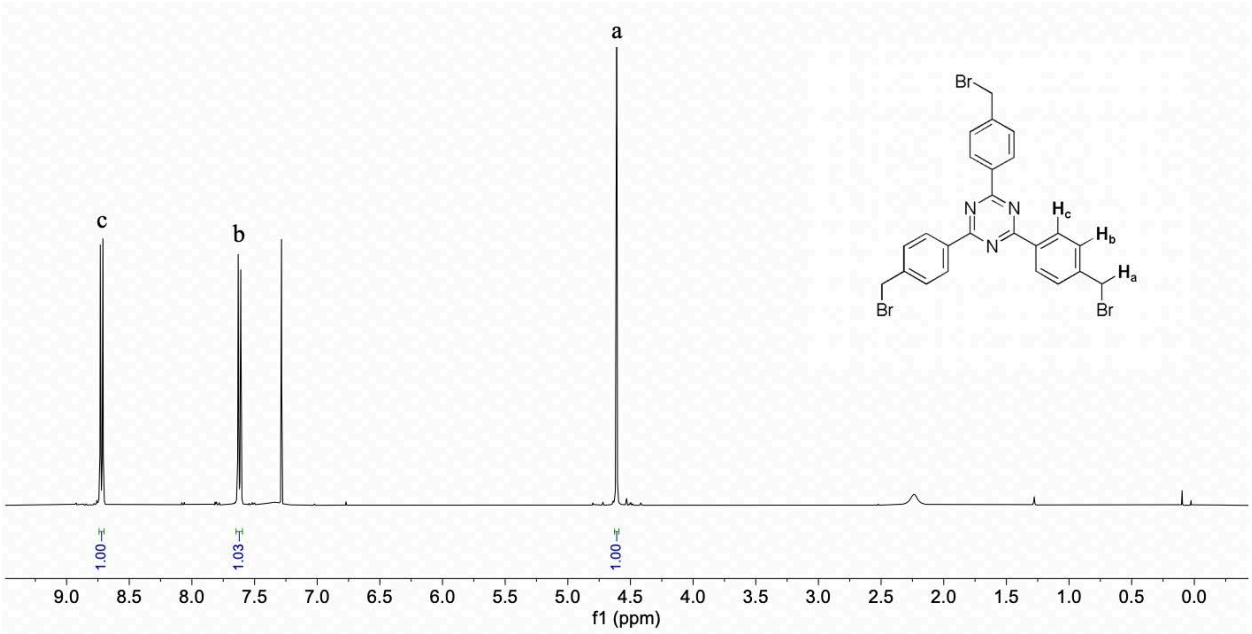

Figure 12 ^{1}H NMR Spectrum of 2,4,6-tris(4-(bromomethyl)phenyl)-1,3,5-triazine **3** ($CDCl_3$, 400 MHz, 298 K).

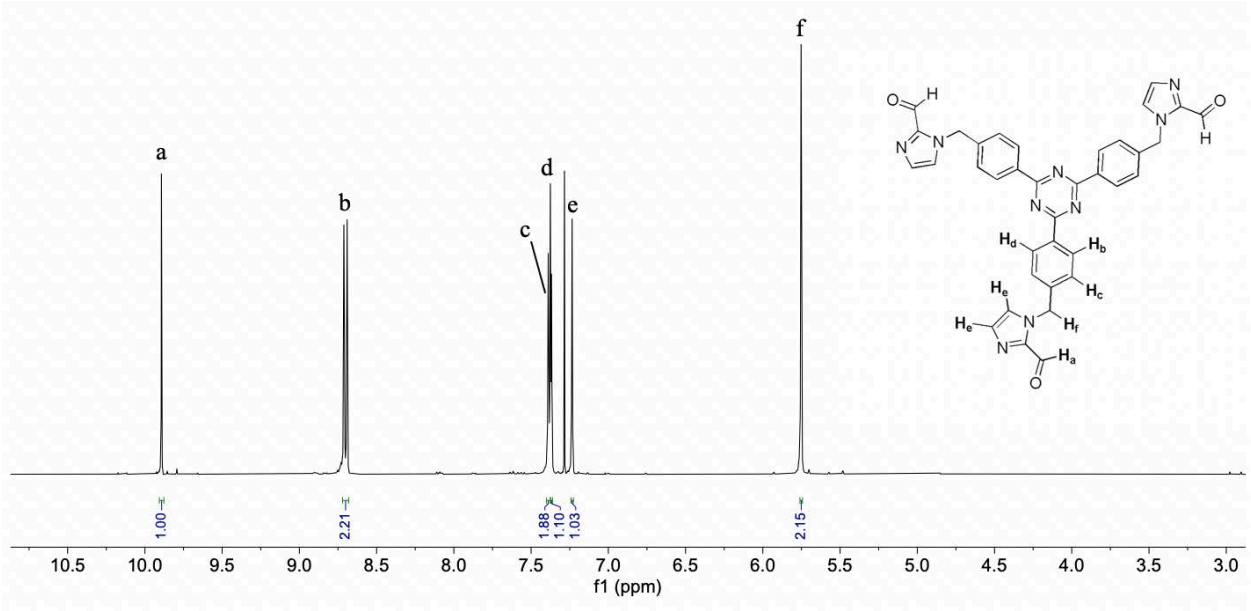

Figure 13 ^{1}H NMR Spectrum of Triimidazole Ligand **4** ($CDCl_3$, 400 MHz, 298 K).

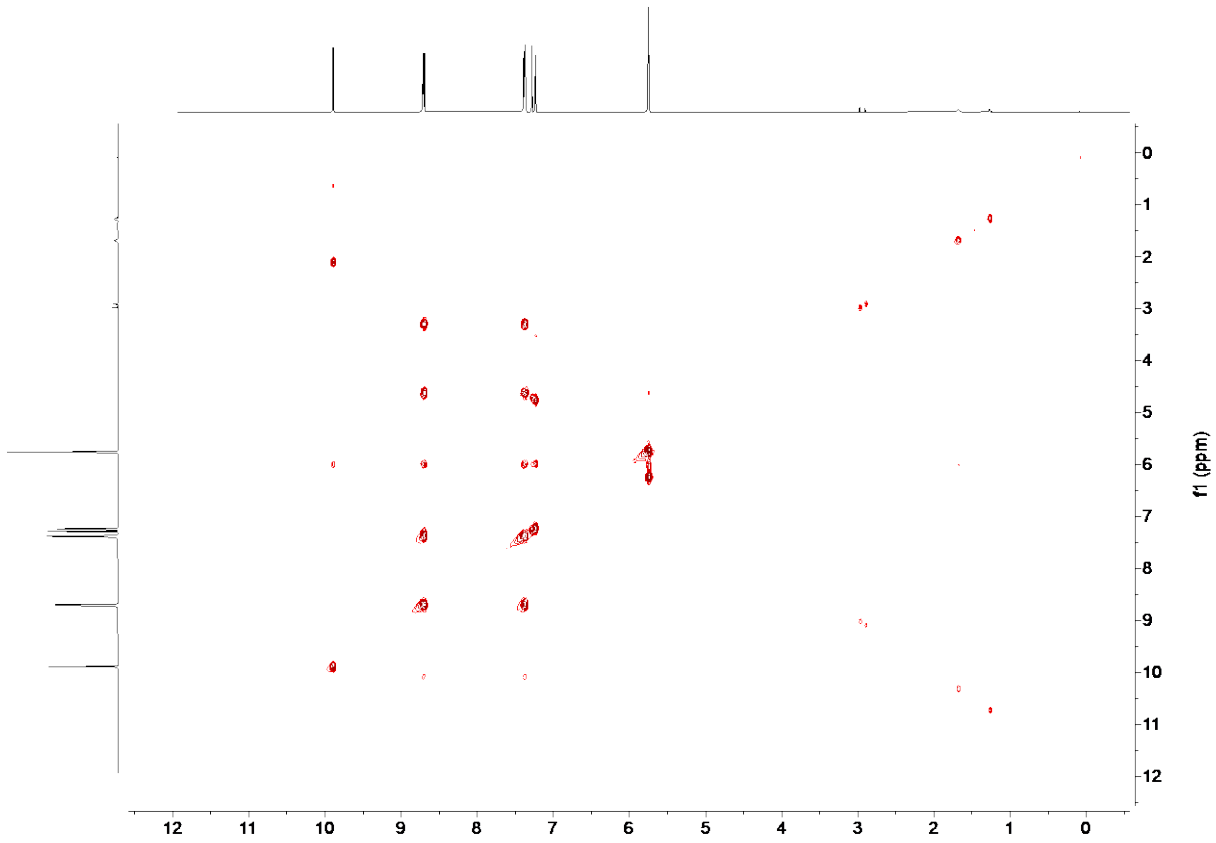

Figure 14 COSY NMR Spectrum of Triimidazole Ligand **4** ($CDCl_3$, 400 MHz, 298 K).

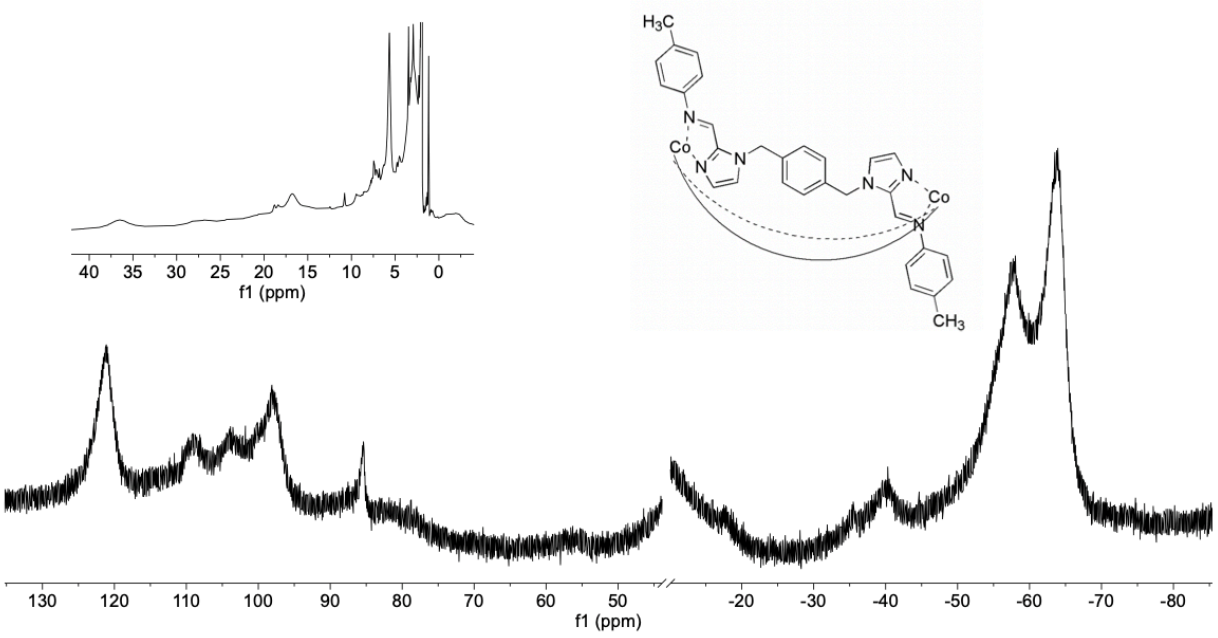

Figure 15 ^{1}H NMR Spectrum of Cage **2•ClO₄** (CD_3CN, 400 MHz, 298 K).

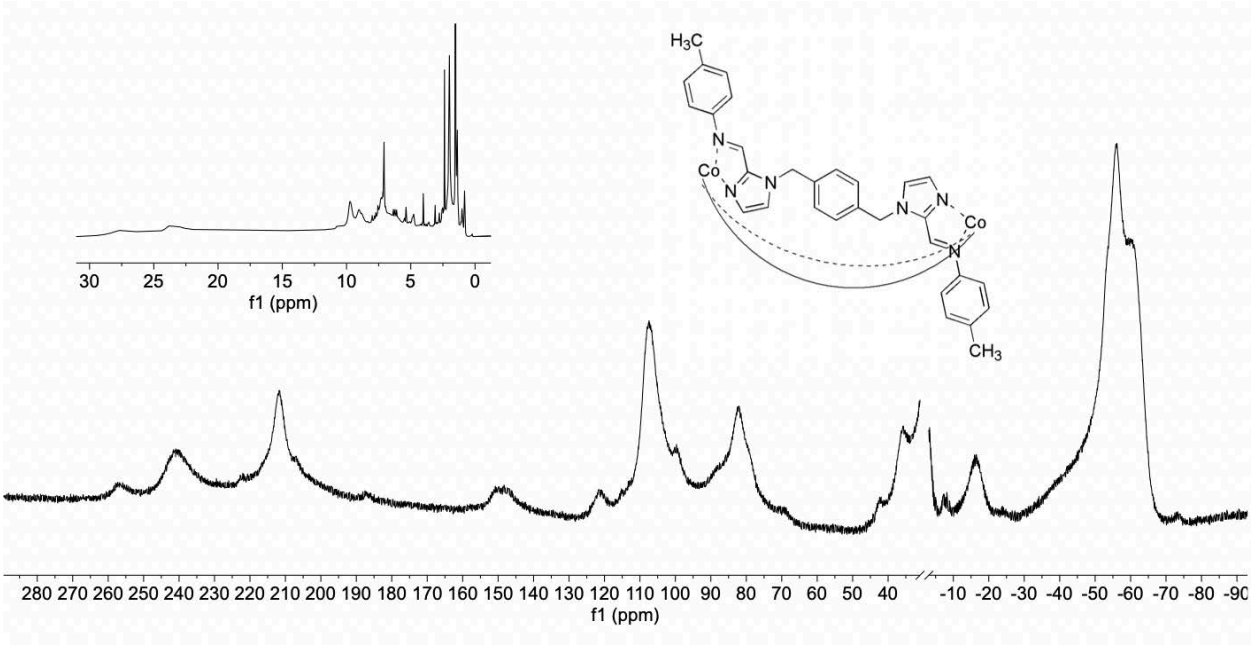

Figure 16 ^{1}H NMR Spectrum of Cage **2•NTf$_2$** (CD_3CN, 400 MHz, 298 K).

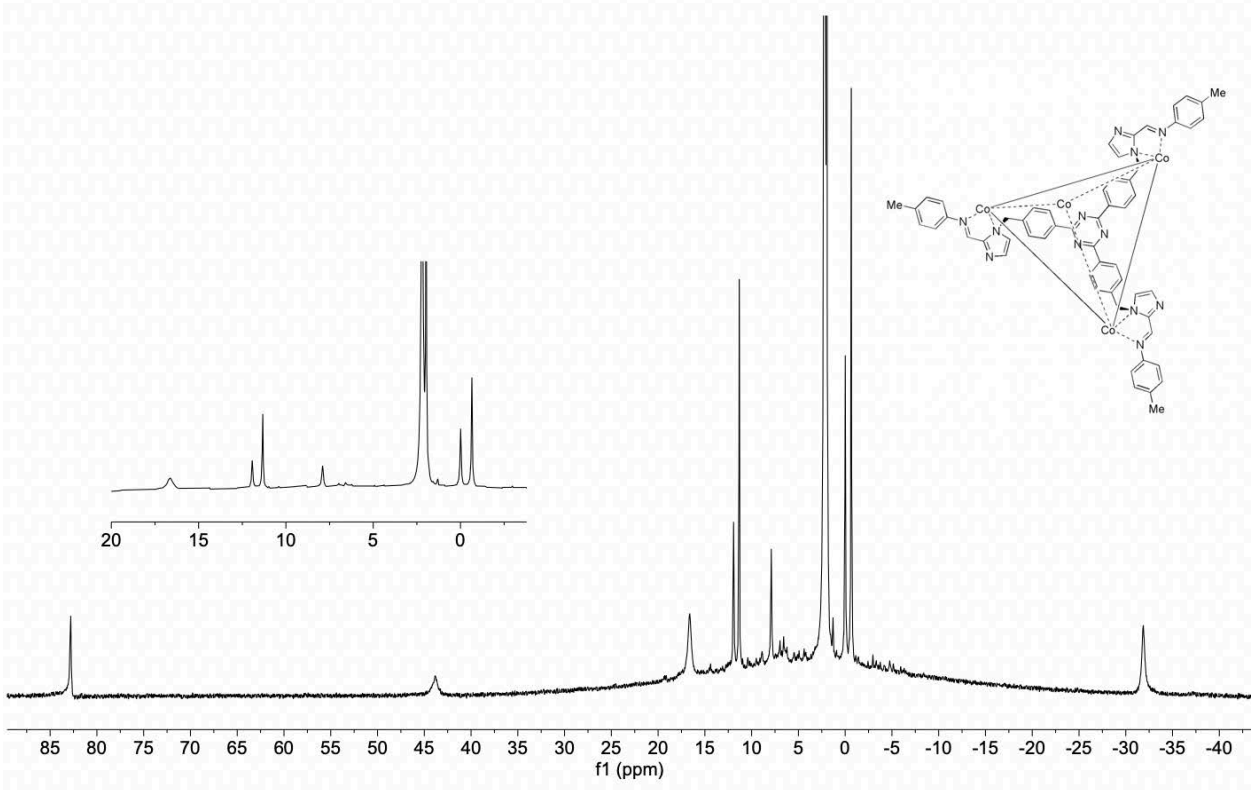

Figure 17 ^{1}H NMR Spectrum of Cage **5•ClO$_4$** (CD_3CN, 400 MHz, 298 K).

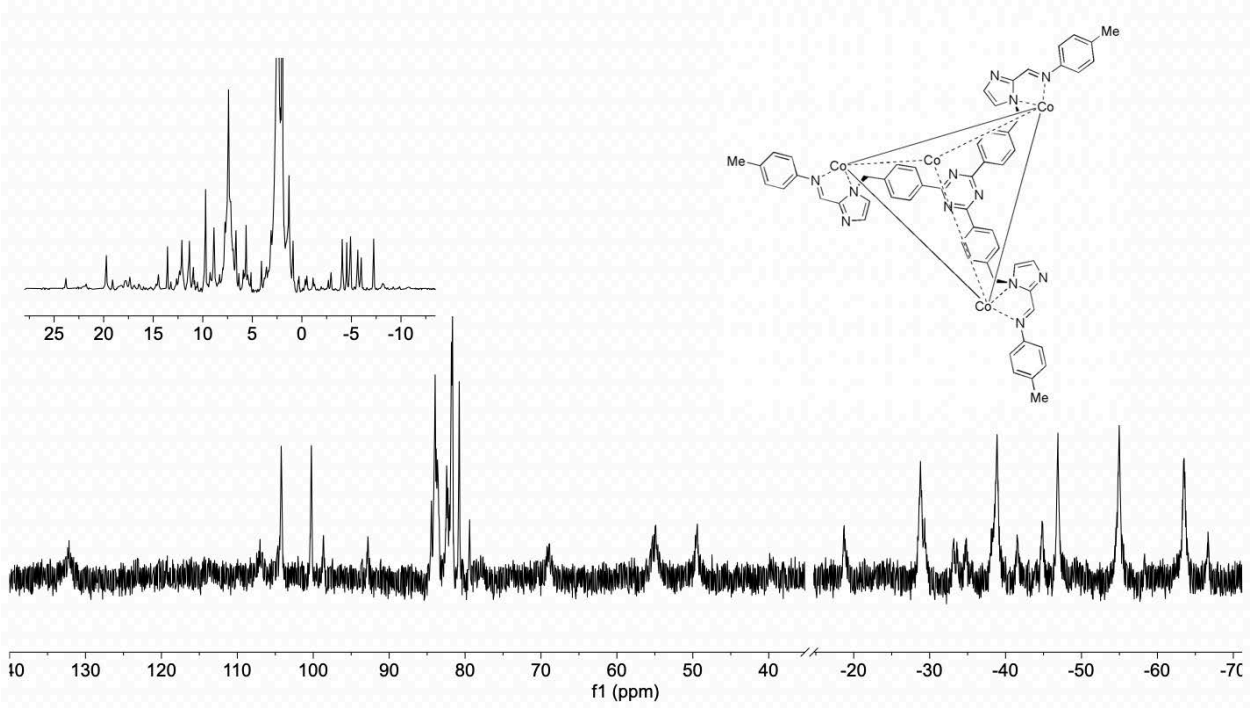

Figure 18 ^{1}H NMR Spectrum of Cage **5•NTf$_2$** (CD_3CN, 400 MHz, 298 K).

References

1. Brown, C.J.; Toste, F.D.; Bergman, R.G.; Raymond, K.N.; Supramolecular Catalysis in Metal-Ligand Cluster Hosts. *Chem. Rev.* **2015**, 115, 3012-3035.
2. He, Q.T.; Li, X.P.; Chen, L.F.; Zhang, L.; Wang, W.; Su, C.Y.; Nanosized Coordination Cages Incorporating Multiple Cu(I) Reactive Sites: Host-Guest Modulated Catalytic Activity. *ACS Catal.* **2013**, 3, 1-9.
3. Mal, P.; Breiner, B.; Rissanen, K.; Nitschke, J.R.; White Phosphorus Is Air-Stable Within a Self-Assembled Tetrahedral Capsule. *Science.* **2009**, 324, 1697-1699.
4. Holloway, L.R.; Bogie, P.M.; Lyon, Y.; Ngai, C.; Miller, T.F.; Julian, R.R.; Hooley, R.J.; Tandem Reactivity of a Self-Assembled Cage Catalyst with Endohedral Acid Groups. *J. Am. Chem. Soc.* **2018**, 140, 8078-8081.
5. Percastegui, E.G.; Mosquera, J.; Ronson, T.K.; Plajer, A.J.; Kieffer, M.; Nitschke, J.R.; Waterproof Architectures through Subcomponent Self-Assembly. *Chem. Sci.* **2019**, 10, 2006-2018.
6. McConnell, A.J.; Spin-state switching in Fe(II) helicates and cages. *Supramolecular Chemistry.* **2018**, 30, 858-868.
7. Mosquera, J.; Ronson, T.K.; Nitschke, J.R.; Subcomponent Flexibility Enables Conversion between D_4-Symmetric $Cd^{II}_8L_8$ and *T*-Symmetric $Cd^{II}_4L_4$ Assemblies. *J. Am. Chem. Soc.* **2016**, 138, 6, 1812-1815.
8. Ward, M.D.; Hunter, C.A.; Williams, N.H.; Coordination Cages Based on Bis(pyrazolylpyridine) Ligands: Structures, Dynamic Behavior, Guest Binding, and Catalysis. *Acc. Chem. Res.* **2018**, 51, 2073-2082.

9. Holloway, L.R.; Young, M.C.; Beran, G.O.; Hooley, R.J.; High fidelity sorting of remarkably similar components via metal-mediated assembly. *Chem. Sci.* **2015**, 6, 4801-4806.
10. Riddell, I.A.; Smulders, M.M.; Clegg, J.K.; Nitchke, J.R.; Encapsulation, storage and controlled release of sulfur hexafluoride from a metal-organic capsule. *Chem. Commun.* **2011**, 47, 457-459.
11. Wiley, C.A.; Holloway, L.R.; Miller, T.F.; Lyon, R.; Julian, R.J.; Hooley, R.J.; Electronic Effects on Narcissistic Self-Sorting in Multicomponent Self Assemble of Fe-Iminopyridine *meso*-Helicates. *Inorg. Chem.* **2016**, 55, 9805-9815.
12. McConnell, A.J.; Spin-state switching in Fe(II) helicates and cages. *Supramolecular Chemistry.* **2018**, 30, 858-868.
13. Morrow, J.R.; Burns, P.J.; Tsitovich, P.B.; Preparation of a Cobalt(II) Cage: An Undergraduate Laboratory Experiment That Produces a ParaSHIFT Agent for Magnetic Resonance Spectroscopy. *J. Chem. Educ.* **2016**, 93, 1115-1119.
14. Tsitovich, P.B.; Cox, J.M.; Benedict, J.B.; Morrow, J.R.; Six-coordinate Iron (II) and Cobalt (II) paraSHIFT Agents for Measuring Temperature by Magnetic Resonance Spectroscopy. *Inorg. Chem.* **2016**, 55, 700-716.
15. Isley, W.C.; Zarra, S.; Carlson, R.K.; Bilbeisi, R.A.; Ranson, T.K.; Nitschke, J.R.; Gagliardi, L.; Cramer, C.J.; Predicting paramagnetic ^{1}H NMR chemical shifts and state-energy separations in spin-crossover host-guest systems. *Phys. Chem. Chem. Phys.* **2014**, 16, 10620-10628.
16. Gu, Z.; Ren, D.; Qiu, D.; Pang, C.; Li, Z.; Chiral tetrahedral iron (II) cages: diastereoselective subcomponent self-assembly, structure interconversion and spin-crossover properties. *Chem. Commun.* **2015**, 51, 788-791.